Scaled Testing to Evaluate Pulse Jet Mixer Performance in Waste Treatment Plant Mixing Vessels - 10487

JA Fort, PA Meyer, JA Bamberger, CW Enderlin, PA Scott, MJ Minette, PA Gauglitz
Pacific Northwest National Laboratory
PO Box 999, Richland, WA 99352

ABSTRACT

The Waste Treatment and Immobilization Plant (WTP) at Hanford is being designed and built to pretreat and vitrify the waste in Hanford's 177 underground waste storage tanks. Numerous process vessels will hold waste at various stages in the WTP. These vessels have pulse jet mixer (PJM) systems. A test program was developed to evaluate the adequacy of mixing system designs in the solids-containing vessels in the WTP. The program focused on non-cohesive solids behavior. Specifically, the program addressed the effectiveness of the mixing systems to suspend settled solids off the vessel bottom and distribute the solids vertically. Experiments were conducted at three scales using various particulate simulants. A range of solids loadings and operational parameters were evaluated, including jet velocity, pulse volume, and duty cycle. In place of actual PJMs, the tests used direct injection from tubes with separate suction at the top of the tank fluid. This configuration provided better control over the discharge duration and duty cycle and simplified the facility requirements. The mixing system configurations represented in testing varied from 4 to 12 PJMs with various jet nozzle sizes. In this way the results collected could be applied to the broad range of WTP vessels with varying geometrical configurations and planned operating conditions. Data for critical suspension velocity, solids cloud height, and solids concentration vertical profile were collected, analyzed, and correlated. The correlations were successfully benchmarked against previous large-scale test results, and then applied to the WTP vessels using reasonable assumptions of anticipated waste properties to evaluate adequacy of the existing mixing system designs.

INTRODUCTION

The Hanford Waste Treatment Plant (WTP) project is applying pulse jet mixer (PJM) technology for tank mixing applications requiring solids mixing, solids suspension, fluid blending, and release of gases generated by radiolysis and thermal processes. PJMs are non-steady jet mixing devices that use compressed air as the motive force. The WTP is being designed and built to pretreat and vitrify the waste from Hanford's 177 underground waste storage tanks. Several process vessels will hold waste at various stages in the WTP. Many of these vessels will have mixing systems with requirements to maintain the waste in a safe condition within the specified operating limits of the equipment.

PJMs are driven by jet pump pairs (JPPs) that use compressed air as the motive force. The suction phase draws process liquid into the PJM from the vessel. The drive phase pressurizes the PJMs via a JPP. This pressurization discharges the PJM liquid at high velocity into the vessel, causing mixing to occur. The drive phase is followed by the vent phase, which allows for depressurization of the PJM by venting through the JPP into the pulse jet vent system. These three phases (suction, drive, and vent) make up the mixing cycle.

The PJMs can be operated in a continuous pulsing mode (e.g., all PJMs on during normal operation) or can be turned off for a time and restarted in the pulsing mode [e.g., for some post-design basis event (DBE) scenarios, vessels that use the 50/50 mixing rack design will only have half their PJMs operational], depending on process requirements. In vessels that contain particulates, solids will settle to the bottom between mixing periods. When the PJMs restart, the settled solids must be resuspended.

The objective of this test program was to evaluate issues related to mixing system designs that could result in insufficient mixing and/or extended mixing times. These issues included a design basis that discounted the effects of large particles and of rapidly settling Newtonian slurries. Geometrically scaled tests were performed with simulants for developing models to be used for confirming the PJM design basis applied to WTP vessels. This test program did not consider cohesive solids behavior that can occur, for example, with small diameter solids at high concentrations, and that has been observed in settled Hanford tank slurries.

Under normal mixing operations, the process areas of concern are solids off-bottom suspension, solids vertical distribution (i.e., concentration profiles), solids accumulation on the vessel bottom, and mixing times. For off-normal mixing operations, the process areas of concern are solids resuspension and overcoming increased rheological properties associated with solids settling. During post-design basis event (DBE) operations vessels may be operated intermittently, with mixing systems idle for 12 hours or longer. Hence, solids settling will occur to varying degrees.

A comprehensive project report has been issued on this work [1]. Additionally specific aspects of this work have been addressed in subsequent conference papers. The scaled experiments are discussed in [2,3] and instrumentation used in the tests in [4]. Following brief background description, this paper describes new correlations that were developed from the data set and shows benchmark results and results of application to the WTP vessels. These correlations and their applications include a number of changes from what

was included in the original project report [1]. Note that the original work [1] was done to a NQA-1 quality standard, the work described in this paper has not been reviewed to that standard and is therefore preliminary.

NOMENCLATURE

C	concentration, solids volume concentration
C(Z)	solids vertical distribution, concentration as a function of elevation
D	diameter of tank
D_{PT}	diameter of pulse tube
DC	duty cycle = t_D / t_C
d	diameter of jet nozzle
d_S	diameter of solids particle
F_{CS}	Froude number at critical suspension
Fr	Froude number = $U^2 / [g\, d(s-1)]$
Fr_p	particle Froude number
f, f′	function
Ga_p	particle Galileo number
g	gravitational constant
H	fluid height, normal fill level
H_C	average peak cloud height
N	number of installed jets or pulse tubes
N_J	number of operating jets/pulse tubes
N_O	number of jets operating in outer ring
R	radial location of PJMs; tank radius
Re	jet Reynolds number = Ud/ν
Re_{CS}	jet Reynolds number at critical suspension velocity = $U_{CS}d/\nu$
Re_p	particle Reynolds number based on particle size and settling velocity = $U_T d_S/\nu$
R_O	radial PJM outer ring location
s	ratio of particle density to liquid density = ρ_s/ρ_l
t_C	cycle time
t_D	drive time, discharge time, pulse time, time at end of pressurization during pulse discharge
t_R	refill time
U	jet velocity
U_{CS}	critical suspension velocity, all solids suspended at the end of the pulse
U_{JS}	jet velocity for off-bottom suspension (jet mixers)
U_{bar}	cumulative average settling velocity
U_T	unhindered terminal settling velocity
U_{TH}	hindered terminal settling velocity
U_0	average velocity
V	nominal volume of tank
V_P	volume of pulse (per PJM)
V_{PT}	volume of pulse tube
V_{REF}	reference volume based on the volume of a right circular cylinder of diameter D where height equals diameter, $V_{REF} = (\pi D^3)/4$
ΔH	level change in fluid height during pulse
ΔL	level change in pulse tube during discharge
ν	kinematic viscosity = μ/ρ_l
μ	viscosity
ϕ	local solids fraction
ϕ_J	jet density = $N_J d^2/D^2$
ϕ_p	pulse volume fraction = $N\, V_P / V_{REF}$
ϕ_{PT}	ratio of pulse tube to vessel cross-sectional area = $N\, D_{PT}^2/D^2$
ϕ_S	ratio of volume of solids particulate to reference volume = $V_S/V_{REF} = V_S/(\pi D^3/4)$
ρ	slurry density
ρ_l	liquid density
ρ_s	solids density

SCALED TESTING APPROACH

In general, mixing system performance for the solids-containing vessels in the WTP depends on the physical and rheological properties of their contents, the number and size of PJMs, vessel size (diameter), and the relative fill level. In addition, mixing performance depends on PJM operating conditions such as jet velocity (U), drive time (t_D), and duty cycle (DC), which is drive time divided by the cycle time (t_C). The scaled testing approach included a series of tests in scaled vessels where these important parameters were varied and measured: relevant similarity criteria; critical suspension velocity (U_{CS}); cloud height (H_C), which is a visible interface above which the fluid is relatively quiescent; and solids vertical distribution C(Z). Mixing times and the distance along the tank bottom over which solids are mobilized by the PJM were not specifically determined. A prototypic PJM mixing system was not used for the experiment, instead a simplified drive system was used that retained the most significant features of the jet discharge and duty cycle. The test system is described further under the Test Design. The details of a prototypic PJM mixing system are described below.

PULSE JET MIXER OPERATION

PJMs differ from mixers that sustain a steady jet to provide mixing. During pulse jet mixing, fluid contained in pulse tubes submerged in the vessel is periodically expelled through the nozzles and into the vessel. This expelled fluid mixes with fluid in the vessel, and solids entrained in the jet are mobilized. While the pulse tubes refill, solids suspended in the fluid may start to settle. This cyclic process is used to suspend, resuspend, and mix particulates contained in the vessel.

Jets are formed by alternating pressure and suction on fluid in pulse tubes coupled to jet nozzles, creating a pulsating flow. The nozzle end of the tube is immersed in the tank, while periodic pressure, vacuum, and venting are supplied to the opposite end. There are three operating modes for the pulse tube: 1) the drive mode, when pressure is applied to discharge the contents of the PJM tube at high velocity through the nozzle; 2) the refill mode, when vacuum is applied to refill the pulse tube; and 3) the vent mode, when the pressure is vented to atmosphere and the pulse tube and tank approach the same fill level. The PJM system uses these operating modes to produce a sequence of drive cycles that provide mixing in the vessel. In the right conditions, multiple pulse tubes, operating either in parallel or in sequence, can be used to effectively provide mixing in liquid/solid systems. The pulse tubes are located in one or two rings at fixed radii from the tank center. The PJMs are distributed uniformly around the vessel circumference.

During the PJM cycle, process parameters affect the degree of mixing and solids motion that occurs. The jet velocity can be used to characterize the state of the solids within the vessel. There are four conditions of note:

1. The velocity at which the particles on the bottom of the tank are all in motion, complete solids suspension or critical suspension velocity (U_{CS}).
2. The cloud height (H_C) at each velocity, should one exist.
3. The jet velocity and pulse cycle for which the solids reach the liquid surface.
4. The PJM operating conditions under which the vertical concentration profile becomes uniform.

A typical PJM system configuration in a vessel is shown schematically in Figure 1. The vessel has diameter (D), volume (V), and fill level (H). There are N pulse jets in the vessel, each with pulse tube diameter (D_{PT}) and volume (V_{PT}). Each PJM has a conical nozzle with exit diameter (d). The volume of fluid expelled during a pulse (V_P) is about 80% of the pulse tube volume to avoid the potential for a pressurized air overblow (i.e., blowing pressurized air from the PJM tubes into the vessel must be avoided). Typically, the total pulse volume ($N \times V_P$) is approximately 5 to 10% of the operating volume of the vessel. During the drive phase the tube is pressurized, and a volume of slurry is discharged. The level change in the tube during discharge is ΔL with a corresponding increase in waste level (ΔH) in the vessel, which is also about 5 to 10% of the operating level, H.

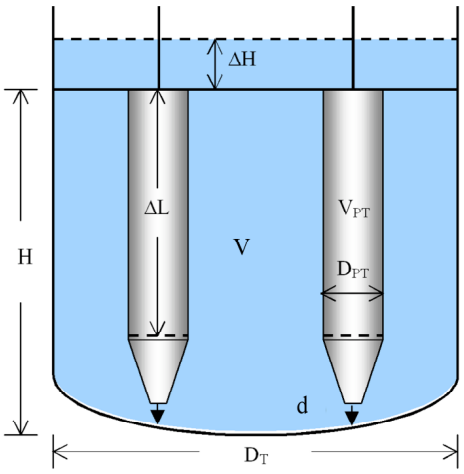

Fig.1. Illustration of a Typical PJM System in a WTP Vessel

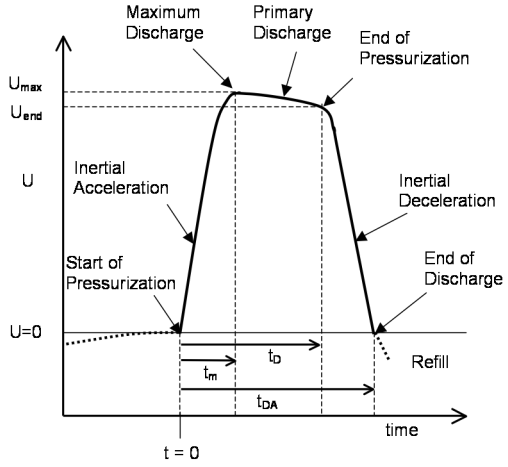

Fig. 2. Illustration of Nozzle Velocity Transient During PJM Discharge

Immediately after the drive phase, a vent is opened, and excess pressure is allowed to vent to atmosphere. During the suction phase, vacuum is applied to the pulse tube, which fills due to a combination of applied vacuum and difference in hydrostatic head between the fluid level and the level in the tube. The refill time (t_R) is the sum of the vent and suction times. The total cycle time for PJM operation is the sum of the drive and refill times ($t_C = t_D + t_R$).

The average drive velocity is averaged both spatially and temporally. Spatially, the velocity varies over the cross section of the nozzle. Temporally, the velocity varies due to transients in the drive pressure and inertial effects. Figure 2 is an illustration of the temporal variation of velocity during one PJM cycle, referred to as a drive function. At the beginning of the drive phase, the fluid inside the PJM is stationary and must be accelerated. When the drive phase is over, some fluid continues to discharge due to the inertia of the moving column of fluid. The inertial effects depend on the physical size of the system. Pulse jet drive functions can vary considerably among mixing vessels in the WTP; mixing system scale, fill level, and slurry properties all have an effect. To compare

PJM systems on a common basis, average velocities should be used with a consistent definition of discharge time. For PJM systems, velocity averages are typically made over the time drive pressure is applied.

EVALUATING MIXING SYSTEMS

The general approach used to evaluate the solids-handling capability of the WTP mixing systems in solids-containing vessels is as follows:

- Develop simulants for noncohesive slurries with properties that bracket anticipated slurry properties in the WTP.
- Perform scaled tests with mixing systems that can be configured to span the geometric and operational parameter space of WTP mixing systems.
- Use well-established metrics to evaluate mixing performance over the testing parameter space.
- Use experimental data to develop models relating mixing performance to slurry properties, geometric parameters, and operational parameters.
- Apply the models to the plant mixing systems, and determine the limiting solids properties the mixing system can handle.
- Assess the acceptability of the limiting solids properties by considering the specific requirements for a given vessel and the percentage of Hanford waste that exceeds the limit. If limiting conditions were deemed unacceptable, the models could then be exercised to evaluate design modifications.

Mixing System Parameters

The primary mixing system parameters shown in Table 1 are slurry properties, mixing system geometric parameters, and operational parameters. Mixing performance in general will depend on the values of these parameters, which can be formed into an equivalent set of dimensionless groups.

Dimensional analysis applied to the physical parameters in Table 1 results in 11 (13 parameters constrained by consistency in three units, mass, length, and time) nondimensional variables when considering single-ring PJM configurations.[1] Double-ring PJM configurations introduce up to two more variables (N_o and R_o/D). The primary nondimensional variables are shown in Table 2. These nondimensional variables are not unique; others can be selected that favor physical insight or specific processes or provide better models of test data. However, they all can be expressed in terms of the physical parameters in Table 1.

Additional nondimensional variables can be formed from parameters in Table 1 that relate to particle settling behavior:

Particle Reynolds number: $Re_p = U_T d_S / \nu = (U_T/U)\,(d_S / D)\,(D/d)\,Re$ (1)

Particle Froude number: $F_p = U_T^2 / g\, d_S$ (2)

Particle Galileo number: $Ga_p = (s-1) g\, d_S^3 / \nu^2 = Re_p^2 / Fr_p$ (3)

Galileo number is referenced without the subscript in the rest of this paper.

Mixing Performance Metrics

The two mixing performance metrics that were evaluated in the experiments and have been correlated for application to WTP vessels are critical suspension velocity and cloud height.

The just-suspended jet velocity, U_{JS}, is defined for steady jet mixing as the discharge velocity required to completely suspend solids that are on the bottom of the vessel. For steady jet mixing, a commonly used criterion is that no solid particles are observed resting on the bottom for more than 1 to 2 seconds. For pulse jet mixing, a reasonable criterion would be that no solids remain on the bottom at the end of the pulse, or, alternatively, that all the solids that have settled during the refill period are completely resuspended during the subsequent pulse. For this study, the velocity to suspend all solids at the end of the pulse is defined as the critical suspension velocity (U_{CS}).

[1] This is true because all single-ring PJM configurations have the same relative radial positioning (R/D). Hence, R/D is not a variable with respect to the plant mixing system designs.

Table 1. Primary Mixing System Physical Parameters

Slurry Properties/Variables	Symbol	Units
Solids diameter	d_S	μm
Solids volume fraction	ϕ_S	(a)
Solids density	ρ_s	g/cm^3
Liquid density	ρ_l	g/cm^3
Liquid kinematic viscosity	$\nu = \mu/\rho_l$	m^2/s
Geometric Configuration	**Symbol**	**Units**
Vessel diameter	D	m (in.)
Nozzle (jet) diameter	d	m (in.)
Number PJMs(b)	N	each
Radial location of PJMs(b)	R	m (ft)
Operational Parameters	**Symbol**	**Units**
Fill level	H	m (in.)
Pulse volume	V_P	m^3
Drive time	t_D	s
Cycle time	t_C	s
Jet velocity	U	m/s

(a) Indicates the parameter is nondimensional.
(b) Includes single and double rings.

Table 2. Mixing System Nondimensional Variables

Slurry Property	Nondimensional Variable
Density ratio	$s = \rho_s/\rho_l$
Solids volume fraction	$\phi_S = V_S/ V_{REF}$ where $V_{REF} = (\pi D^3)/4$
Particle diameter ratio	d_S/D
Geometric Properties	
Nozzle diameter ratio	d/D
Number of pulse tubes	N
Jet density	$\phi_J = N_J(d/D)^2$
PJM location	R/D
Ratio of pulse tube to vessel cross-sectional area	$\phi_{PT} = N(D_{PT}/D)^2$
Operational Parameters	
Fill level	H/D
Pulse volume fraction	$\phi_p = N V_P/ V_{REF}$ where $V_{REF} = (\pi D^3)/4$
Duty cycle	$DC = t_D / t_C$
Jet Reynolds number	$Re = U d / \nu$
Froude number	$Fr = U^2 /g d(s-1)$

In general it can be expected that U_{CS} is a function of the important mixing parameters. This is expressed mathematically by

$$U_{CS} = f(d_S, \rho_s, \rho_l, \phi_S, \nu, D, d, N, V_P, R, H, t_D, t_C) \quad (4)$$

The critical suspension velocity can also be expressed in terms of the (dimensionless) Froude number as

$$F_{CS} = U_{CS}^2 / [g\, d(s-1)] = f'(s, \phi_S, d_S/D, d/D, N, R/D, H/D, \phi_p, DC, Re_{CS}) \quad (5)$$

This Froude number can be interpreted as the ratio of jet kinetic energy to the potential energy required to suspend the mass of settled solids one particle diameter in elevation.

A power law is suggested as the functional form of f′ in Eqn. (5). This is based on the form of an industrial correlation proposed by Zwietering (1958) for bladed mixer performance [5].

During mixing system operation, solids will become suspended off the bottom of the vessel. For continuous mixing, the solids fraction will achieve a stable distribution. With pulse jet mixing, changes in solids concentration may occur between pulses. By either assuming quasi-steady solids distributions, or by averaging over a drive cycle, the solids fraction vertical distribution can be expressed mathematically as

$$\phi / \phi_S\,(Z/D) = f(s, \phi_S, d_S/D, d/D, N, R/D, H/D, \phi_p, DC, Re, Fr) \quad (6)$$

where ϕ is the local solids fraction and Z/D is the normalized vertical elevation. For some conditions a distinct interface forms at a certain vertical elevation with no solids suspended above. This is referred to as the cloud height (H_C). The cloud height can also be expressed in terms of the mixing parameters.

TEST DESIGN

Details of the Test Design and example test data are provided in [1]. This section briefly summarizes factors and considerations involved in the experimental test design, specifically as related to producing an applicable dataset for predicting rating metrics for full-scale WTP vessels.

Approach

The following test design approach was used to ensure that robust models for rating metrics would be achieved by the test program.

- The conditions tested bracketed plant nondimensional parameter ranges to the extent practical.
- Testing occurred at three scales to establish scale-up.
- Test variable ranges were extended so that test results are applicable to evaluating design improvements (such as large nozzles, more pulse tubes, etc.).
- Sufficient data were collected to develop models for rating metrics that, when applied to plant vessels, have reasonable uncertainty.
- Jet discharge characteristics were the same at all scales.
- The same instrumentation and measurement methods were used at all scales.

Plant Variable Ranges

Table 3 gives a summary of the ranges of nondimensional variables associated with WTP mixing systems. The test parameter ranges were designed to bracket these conditions and ranges of variables for completed experiments are shown for comparison.

Selection of Slurry Property Ranges

Solid particle simulants were selected to permit evaluation of mixing performance over a range of operating conditions. Physical properties of density and size distribution were considered. Initial particles selected were commercially available glass beads with a relatively broad size distribution. Initial tests were conducted with these solids. To gain additional insight into the effect that the size distribution of the initial simulant on mixing parameters, particles with a much narrower size distribution were selected for the focused tests. The testing system limited the use of very small and low density particles because these particles would be removed from the testing tank by the pump inlet at the top of the tank. The property ranges for these simulants are included in Table 3, where values bound the ranges used during testing with noncohesive simulants.

Scaled Vessels and Test Mixing System

Tests were conducted in three test systems (small-, mid-, and large-scale) using acrylic tanks with diameters of 0.367, 0.86, and 1.78 m (14-7/16, 34, and 70 in.), respectively. Four different test tank head[2] (bottom) profiles were prepared: flat, 100-to-6 flanged and dished, semi-elliptical, and spherical.

The differences in tank head profiles result in different impingement angles between the vertical jet and the tank head. For the outer ring of PJMs, the differences in tank head profiles result in significantly different impingement angles at the same radius from the center. To duplicate the impingement angle of a flanged and dished configuration (e.g., as used in the HLP-22 vessel), the radial location of the outer PJM ring was changed to match that impingement angle in the elliptical configuration.

To simplify and expedite the testing, the test apparatus was designed with a closed-loop, pumped-jet system with the pump return line near the liquid surface. Pulsation of the discharge flow was achieved by valve operation. There are several aspects of this system that are non-prototypic of a PJM mixing system:

- PJMs are replaced by smaller diameter tubes with straight-bore nozzle inserts

[2] The tank "head" is the bottom surface of the tank. For the small- and mid-scale tanks, the head is integral to the tank. For the large-scale tank, the head is interchangeable by attaching the acrylic tube to the either the flanged and dished or elliptical head.

- Fluid is discharged from the tube inserts during drive but is not withdrawn into the tube during suction
- Fluid height in the vessel is maintained by a suction outlet at an elevated fluid height during the discharge from the nozzles
- Discharge from the tube nozzles was accomplished by servo valve control

Table 3. Preliminary Bracketing Noncohesive Property Ranges

Property	Symbol	WTP Vessel Range	Test Vessel Range
Slurry Properties			
Solids diameter	$\mathbf{d_S}$	10-1000μm	44-766μm
Solids volume fraction	$\boldsymbol{\phi_S}$	0.001-0.15	0.00015-0.06
Density ratio	$\mathbf{s = \rho_s / \rho_l}$	1.5-11	2.45-4.18
Solids density	ρ_s	*2.2-11 g/cm³*	2.45-4.18 g/cm³
Liquid density	ρ_l	1-1.4 g/cm³	1.0 g/cm³
Slurry density	ρ	1-2.7 g/cm³	
Viscosity	μ	*1-25 cP*	
Kinematic viscosity	$\nu = \mu/\rho_l$	7.10E-07-2.50E-05 m²/s	
Settling velocity	U_T	*1.10E-6-0.18 m/s*	0.0017-0.11 m/s
Galileo number	$Ga_p = (s-1)g\, d_S^3/\nu^2$	7.80E-06-1.90E+05	
Particle Reynolds number	$Re_p = U_T\, d_S/\nu$	4.40E-07-7.30E+02	
Particle Froude number	$F_p = U_T^2/(g\, d_S)$	2.40E-08-2.80E+00	
Geometric Configuration			
Vessel diameter	**D**	9.5-47 ft	14 7/16-70 in.
Nozzle diameter ratio	**d/D**	0.007-0.07	0.126-0.92 in.
Number PJMs	**N**	1-12	4, 8, 12
Number of PJMs in inner ring	$\mathbf{N_I}$	0-4	0, 4
Number of PJMs in outer ring	$\mathbf{N_O}$	0-8	4, 8
Operational Parameters			
Fill level ratio	**H/D**	0.32-1.6	1.25-2.51
Drive time	t_D	5.4-79 s	
Duty cycle	**DC**	0.23-0.37	0.14-1.0
Pulse volume fraction	$\boldsymbol{\phi_p}$	0.0039-0.13	0.025-0.15
Jet velocity	**U**	8-13 m/s	0.8-14.7 m/s
Reynolds number	$Re = U\, d\, /\, \nu$	3.30E+04-3.40E+06	
Froude number	$Fr = U^2/(2g\, d)$	0.3-2.3	
Particle ratio	d_S/d	4.90E-05-9.80E-03	

For mobilization of solids on the tank floor, floor shear predictions from CFD show that the straight-bore nozzles provide conservative results at lower discharge velocities in which the radial clearing of solids from the tank floor is less than that required for the critical suspension velocity to be achieved. As the discharge velocity is increased and solids mobilization is achieved at higher radial distances, the differences in solids mobilization obtained for conical and straight-bore nozzles are predicted to become negligible.

The smaller diameter of the tubes occupies a smaller portion of the vessel volume, but this is considered to have a negligible impact on the solids suspension. The fluid discharge is better controlled with servo valves, and the velocity drive function is more of a "top-hat" profile than typical PJMs. Again, this is not significant in terms of mixing; however it is important to compare average velocities from this profile to the prototypic systems. This will be discussed further in the Benchmarks section. Arguably the most significant difference between the test drive system and a prototypic PJM driven system is the substitution of a suction outlet at the top of the vessel for the suction phase of the PJM drive cycle. Although small, this introduces a net upward velocity in the tank that may enhance solids suspension. Also, the effect of discharging clear fluid means that the jet can be less dense and consequently have less momentum than a solids laden jet from a PJM. The net effect of all these non-prototypic features in the drive system was believed to be small relative to the dominant effect of solids suspension due to the fluid jet portion of the drive cycle.

TESTING OVERVIEW

The experimental procedures used during the scaled mixing experiments are described in this section. The experiments were conducted in two test campaigns: initial and focused. During each test campaign, improvements in testing protocol and instrumentation were implemented. However, the overall goal of the testing remained the same: to determine the U_{CS} for each test and to determine the cloud height at a range of velocities surrounding U_{CS}.

The main test objective was to observe the influence of vertically downward-directed jets on noncohesive solids in a series of scaled tanks with several bottom shapes. The test tanks and bottom shapes included small-and large-scale tanks with elliptical bottoms, a mid-scale tank with a spherical bottom, and a large-scale tank with a flanged and dished bottom.

During testing, the downward-directed jets were operated in either a steady flow condition or a pulsed (periodic) flow condition. The mobilization of the solids resulting from the jets was evaluated based on:

- The motion/agitation of the particulate on the tank floor
- The elevation the solids reach within the tank (the combination of jet velocity and duty cycle was kept low enough that the solids interface, or cloud height, was observable and well below the suction outlet).
- Other observations deemed significant to characterize the system performance relative to mobilization and/or suspension of solids, such as patterns and dimensions of the cleared regions of the tank floor where particulate had been swept away. In the focused tests, measurements of the solids concentration profile were collected using ultrasonic attenuation methods.

Details of test procedures and instrumentation used are provided in [1,2,3,4].

ANALYSIS

Performance Metric Models

The updated models differ from the originals in [1], in part, because several test conditions were removed from the correlation dataset after consideration of return line inlet height. The updated models described here are new versions of the physical model that was identified in the original report [1]. New features in each model are summarized next.

U_{CS} Model

Other than constraints imposed on the fit coefficients and the use of the modified dataset, the U_{CS} model is unchanged. Coefficients and exponents are different than in [1], but the form is the same. Specifically, the exponents on ϕ_p and ϕ_J were allowed to vary unconstrained from those in the H_C model. In the previously reported models[1], these exponents were the same in both. There is no reason they needed to be the same. The exponent on Ga was also allowed to vary in an effort to improve the fit. It was previously set to 0.5, which was a value cited in [1] as being consistent with power required to maintain solids suspension. The optimized coefficient is sufficiently close to not disallow this argument. Finally, the "hindered" settling exponent is now set equal to 6 and the max concentration is set to the experimentally measured value of 0.6 instead of previously used value of 0.5.

The result is

$$\frac{U_{CS}}{U_{TH}} = 2.302\left(D^* / Ga^{0.673}\right)^{0.261} \tag{7}$$

where

$$D^* = \frac{D(s-1)g\phi_s}{DC\ U_{TH}^2 \phi_p^{0.898} \phi_J^{1.958}} \tag{8}$$

$$U_{TH} = U_T\left(1 - \frac{\phi_S}{0.6}\right)^6 \tag{9}$$

Correlation results for U_{CS} are shown in Figure 3.

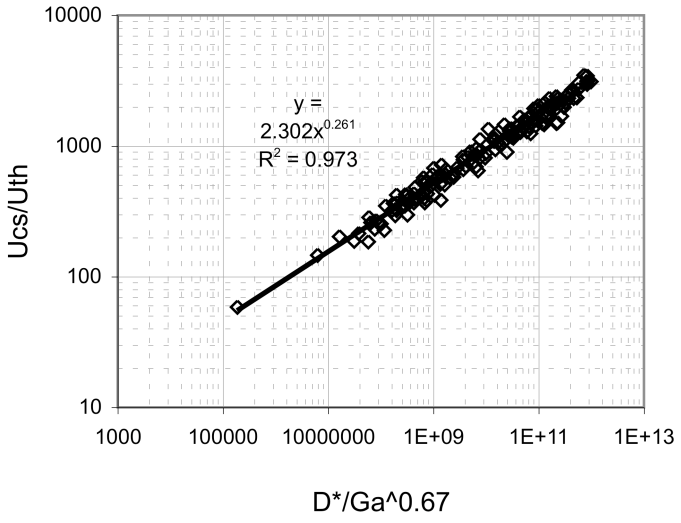

Fig. 3. Data correlation for U_{CS}

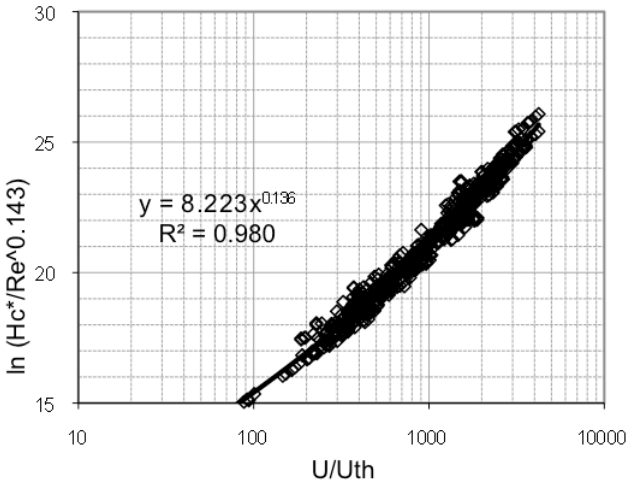

Fig. 4. Correlation for $\ln(H_C^*)$

H_C Model

A significant change in this new version of the H_C model was to include the number of tubes, N, as an independent parameter. Many of the cloud height data points showing poor agreement with the model in the project report [1] were for 8 and 4 tube tests. This pointed to insufficient functionality for N, which the current model is intended to correct. As in the U_{CS} model, the exponents on ϕ_P and ϕ_J were allowed to vary independently. The exponent on Ga was allowed to vary, but was found to be very small (<0.05); hence it was set to zero (not included) in the final model. The same "hindered" settling expression is used in both U_{CS} and H_C models. Finally, a jet Reynolds number term was added to account for geometrical scale.

The result is

$$\ln\left[H_C^* \, Re^{-0.143}\right] = 8.223\left(\frac{U}{U_{TH}}\right)^{0.1364} \tag{10}$$

where

$$H_C^* = \frac{H_C(s-1)g\phi_S N^{0.658}}{DC - U_{TH}^2 \phi_P^{0.898} \phi_j^{1.662}} \tag{11}$$

Note the inclusion of Re results in $H_C \sim d^{0.14}$. For geometric similarity d varies as D for a given test, thus the cloud height varies as (system size)^(0.14).

Correlation results for $\ln(H_C)$ are shown in Figure 4. For this model the comparison of model prediction versus measured H_C is substantially better than was observed with the previous physical model [1].

Benchmarks

The new models were used to update the benchmark comparisons in [1] between model predictions and measured results in the three experiments with prototypic PJM mixing systems. These experiments are described in their individual reports [6, 7, 8]

Several changes were made in the process of updating these benchmark comparisons. The first change was to more consistently represent the prototypic PJM driven experiments in the model inputs with the representation of operational parameters from the non-prototypic driven experiments upon which the model is based. Specifically, this required adjustments to the PJM duty cycle and drive velocity used for the benchmarks. Figure 5 illustrates a typical drive cycle and definition of duty cycle used in the scaled experiments. The target drive velocity is also shown in this figure and is clearly represents the average of the maximum drive velocity. In PJM calculations, we have typically averaged over the time the drive pressure is on. This then includes the ramp-up portion of the drive profile in the average velocity calculation, which lessens the computed average over what was used in the scaled tests (Figure 5). The duty cycle typically computed for PJMs is equal to the time that drive pressure is applied divided by total cycle time. In Figure 5, it can be seen that the duty cycle used for scaled experiments includes the ramp down time as well. Thus looking at the benchmark experiments with the perspective of using definitions consistent with the scaled experiments, we found that benchmark experiment drive velocities and duty cycles should be increased. The drive velocity for the filtration simulant (FS) benchmarks is left unchanged since we do not have any measured drive function for that experiment [6]. The 8 m/s value used in that case was a rough estimate based on later experience at the recorded (4 bar) drive pressure. The updated drive velocities and duty cycles for each benchmark are shown with other input values in Tables 4 through 6.

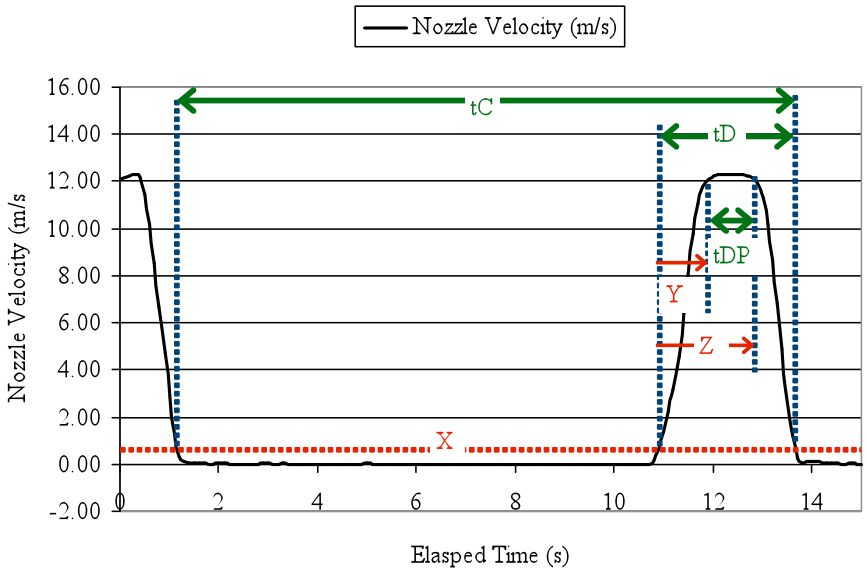

Fig. 5. Drive profile characterization in scaled experiments. X, the setpoint, is a threshold velocity for distinguishing assumed zero flow condition and measured flow. A pulse or discharge pulse is that portion of the cycle for which the velocity is greater than X. t_D is the discharge or pulse time and t_{DP} is the time over which the target velocity is calculated or observed.

The second change was to employ a systematic approach to determine two representative settling velocities for each benchmark. One value, the favorably conservative bound, produced a concentration at the floor that matched that of the lowermost concentration measurement from the experiment. The second, best estimate, matched the floor concentration that was would account for the total mass in the system.

Table 4. Updated model inputs for Tests with AZ-101/102 Filtration Simulant [6]

Case #	% Max Drive	wt% Solids	ϕ_S	DC	ϕ_p	ϕ_J	H/D	U (m/s)
1	100%	17.6	0.044	0.33	0.077	0.0027	0.82	8
2	50%	17.6	0.044	0.167	0.077	0.0027	0.82	8
3	10%	17.6	0.044	0.033	0.077	0.0027	0.82	8
4	100%	28.3	0.082	0.33	0.077	0.0027	0.86	8
5	50%	28.3	0.082	0.167	0.077	0.0027	0.86	8
6	10%	28.3	0.082	0.033	0.077	0.0027	0.86	8

Table 5. Updated model inputs for Tests with 75-μm Glass Beads [7]

Case #	Case	wt% Solids	ϕ_S	DC	ϕ_p	ϕ_J	H/D	U (m/s)
7	4 PJMs	10	0.042	0.20	0.056	0.0027	0.99	7.2

Table 6. Updated model inputs for Tests with 35-μm Glass Beads [8]

Case #	Case	wt% Solids	ϕ_S	DC	ϕ_p	ϕ_J	H/D	U (m/s)
8	4 PJMs	20	0.085	0.31	0.070	0.0027	0.93	9.7
9	2 PJMs	20	0.085	0.30	0.036	0.0014	0.93	9.3

The favorably conservative bound is unambiguous and is obtained directly from the experimental data. Its accuracy is that of the measurement and its representativeness of what was on the tank floor is partly a function of the distance the measurement above the floor and also a function of the measurements discernment of lateral distribution. Benchmark experiments differed in measurement position minimum heights and in measurements off of centerline.

The best estimate condition must be calculated using the measured concentration data. A simple stepwise integration was used, beginning at the floor, with concentration held fixed between measurement elevations. The accuracy of the floor concentration in this case was subject to this integration and the ability of the limited measurement locations to resolve the actual concentration profile. Several cases produced best estimate conditions that were not plausible, most often being far smaller than the favorably conservative bound.

For convenience in the plotted and tabular results, we will use $w_{0\,min}$ to refer to the favorably conservative bound and $w_{0\,max}$ to refer to the best estimate condition. The $w_{0\,min}$ and $w_{0\,max}$ concentrations calculated for each benchmark experiment are summarized in Table 7. The italicized values shown in Table 7 for the best estimate condition (w_{0max}) are implausible since floor concentrations will likely always be higher than the measured value at lowest elevation.

Table 7. Favorably conservative bound ($w_{0\,min}$) and best estimate ($w_{0\,max}$) floor concentrations for benchmark experiments

mass fraction at floor	FS #3	FS #6	FS #14	FS #19	FS #20	FS #28	Glass 75 mm	Glass 35 mm 2 PJM	Glass 35 mm 4 PJM
$w_{0\,min}$	0.178	0.200	0.259	0.270	0.306	0.367	0.284	0.357	0.220
$w_{0\,max}$	0.209	0.239	0.422	0.412	***0.288***	0.553	***0.252***	***0.234***	***0.074***

The linear concentration profile model is used unchanged from the previous analysis. Sample benchmark comparisons for one case are shown plotted in Figure 6 illustrating the concentration profile with value at the floor matching the target values. This sample is also significant as it is the result for the 75 μm glass benchmark. Figure 7 compares the settling velocity distribution for the 75 μm glass with the other benchmark experiment simulants, the scaled test simulants and with the Case 3 Hanford particle size and density distribution (PSDD). The 75 μm glass simulant has a narrow size distribution that is more typical of the scaled test simulants, thus we would expect it to be more closely represented by the volume average settling velocity, U_{bar}. As the dashed line profile shows in

Figure 6, U_{bar} is a reasonably good fit to the concentration profile. The max floor concentration is not available (this is one of the points shown italicized in Table 7) so no conclusion can be made about how the model with U_{bar} matches that parameter.

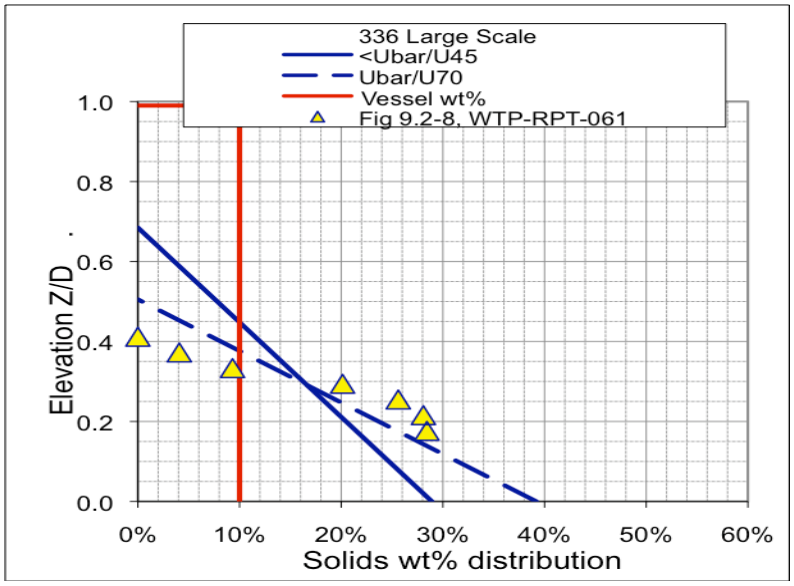

Fig. 6. Sample benchmark results illustrating concentration profile and values at floor matching min and max targets

Settling velocities U_{Tmin} and U_{Tmax} used to match the w_{0min} and w_{0max} floor concentration targets for individual benchmarks are listed in Table 8. These values were then used with the respective PSDs or PSDDs for the experiment to determine percentiles and cumulative percentile ($U_{bar\ n}$) settling velocities[3]. For the filtration simulant benchmark the PSDD has been updated to use the measured PSDs of each component. These measured PSDs were provided in support of settling velocity tests for this simulant in [7]. PSDs for the two glass bead simulant benchmarks are unchanged. The percentiles are shown along with the settling velocities in Table 6. Again, the settling velocities obtained for the problematic points are shown italicized.

Table 8. Settling velocities required to match benchmark concentration targets

Velocity (mm/s)	FS #3	FS #6	FS #14	FS #19	FS #20	FS #28	Glass 75 mm	Glass 35 mm 2 PJM	Glass 35 mm 4 PJM
$U_{T\ min}$	**1.1**	**1.5**	**0.92**	**1.7**	**1.4**	**0.94**	**3.6**	**4.2**	**3.8**
Percentile	0.86	0.89	0.83	0.91	0.89	0.83	0.39	0.92	0.91
$U_{bar\ n}$	0.30	0.47	0.13	0.54	0.45	0.15	0	0.75	0.70
$U_{T\ max}$	**2.5**	**2.0**	**1.2**	**3.3**	*2.8*	**1.2**	*4.7*	*4.7*	*4.5*
Percentile	0.93	0.92	0.87	0.95	0.94	0.87	0.66	0.93	0.93
$U_{bar\ n}$	0.69	0.60	0.34	0.78	0.73	0.34	0.01	0.79	0.78

[3] Here $U_{bar\ n}$ is used to refer to a U_{bar} value at a specific cumulative percentile beginning at the maximum settling velocity ($U_{bar\ 100}$). In this case $U_{bar\ 0}$ is the volume average settling velocity for the entire PSDD and is just referred to as U_{bar}. See the original reference [1] for details.

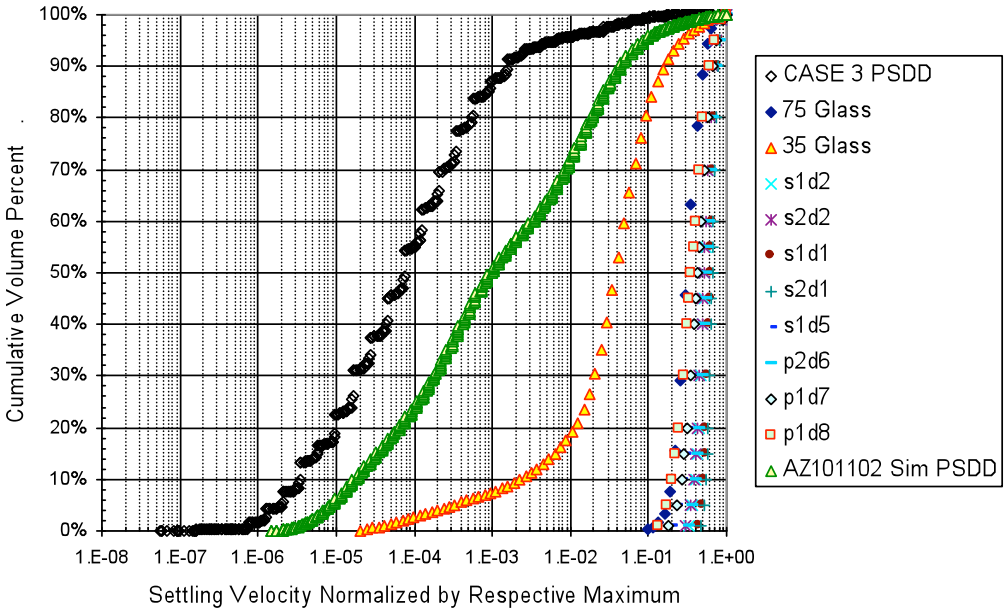

Fig. 7. Comparison of settling velocity distributions between Hanford Case 3 PSDD, scaled tests and benchmark experiment simulants (the filtration simulant is labeled AZ101/102 Sim).

As a final step in the benchmarking exercise, average percentiles are computed for the to determine settling velocities, U_{T1} = avg ($U_{T\ min}$) and U_{T2} = avg ($U_{T\ max}$), that will be used in the WTP vessel applications. In computing these averages we consider several possible cases. The 75 μm glass benchmark data is excluded from all cases since it is more typical of a monodisperse simulant and our goal in the averaging process is to determine settling velocity percentile that represents behavior of a broad spectrum polydisperse PSDD slurry in the WTP vessels (see Figure 7). The cases considered are: 1) all filtration simulant and 35 μm glass simulant benchmarks, 2) all benchmarks except the low duty cycle filtration simulant cases (FS #14 and #28), and 3) all benchmarks except the low duty cycle and italicized points in Table 8. The low duty cycle cases are excluded because they are far out of range of the scaled test experiments and WTP vessel applications. The problematic benchmarks (shown italicized in Table 8) are excluded because we have no clear basis for w_{0max}, as mentioned previously. For each case, a simple average results in the pair of settling velocities in Table 9. Note that average percentiles are not included in this table, only cumulative percentiles ($U_{bar\ n}$) since these are the most appropriate values for representing different PSDDs in this application. Of the three cases shown, the most appropriate is the third, which gives U_{bar53} for the average conservative bound and U_{bar69} for the best estimate. As in [1], the WTP vessel applications use the Case 3 Hanford PSDD with liquid density of 1.1 Sp.G. and viscosity of 1.5 cP. For these conditions U_{bar53} is 2.2 mm/s and U_{bar69} is 3.3 mm/s. The minimum falls between U_{94} and U_{95} and the maximum between U_{95} and U_{96}. So as in the initial estimate described in Section 10.3 of [1], the conservative bound and best estimate settling velocities bracket the U_{95} settling velocity (U_{95} is 2.5 mm/s). WTP vessel applications are presented in the next section for U_{bar53} and U_{bar69}.

Table 9. Average cumulative percentile settling velocities

	All benchmarks (except 75 μm glass)	Excluding low DC FS cases	Excluding low DC FS and italicized points in Table 8
U_{T1} = avg $U_{bar\ n\ min}$	0.40	0.53	0.53
U_{T2} = avg $U_{bar\ n\ max}$	0.63	0.73	0.69

Model Applications to WTP Vessels

Geometry and operational data are unchanged from the cases used in the report (see Tables 9.2 and 9.4 of [1]). Only the Hanford PSDD cases are included in the analysis in this section of the paper. The use of the Hanford Waste Tank characteristics is most significant for the initial vessels receiving wastes from the tank farms. As leaching, filtering and washing of the waste occurs the characteristics of the wastes in latter vessels change significantly. All results for this comparison and for subsequent results are for the maximum vessel fill level.

Results of the model applications for the selected min and max average percentile settling velocities ($U_{T1} = U_{bar53}$ and $U_{T2} = U_{bar69}$) for a range of WTP solids containing vessels are presented in Figure 8. The ratio of design velocity to the critical suspension velocity, U/U_{CS}, is shown in Figure 8a. Where this value is shown to be greater than one, the design nozzle discharge velocity is adequate to suspend the solids off the vessel floor, for the particle settling velocities indicated and the vessel design conditions (solids loading, PJM mixing parameters and vessel fill level). Values shown less than one indicate that the design velocity is inadequate to move all of the solids from the vessel floor. The ratio of cloud height to fill height, H_C/H_f, is shown in Figure 8b. In this case, values one represent a design where particulate suspension levels would just reach the vessel fill level. Since concentration increases from a minimum at the top of the cloud to maximum at the bottom of the vessel, $H_C/H_f=1$ still implies a majority of the solids in the bottom half of the vessel. Therefore $H_C/H_f=1$ represents a minimum requirement for the vessel. Values well above this are reasonably well-mixed, and values well below this are inadequate, again given these particulate settling velocities and vessel design parameters. Note that very small and very large values ($1>H_C/H_f > 10$) reflect limits of the model assumptions are not physically meaningful, except that they represent a mixing system that is either far underpowered (for very small values) or a system that has excess mixing capacity for these conditions. Finally, the pump suction metric, $0.2/C_0$, is shown in Figure 8c. This represents the predicted solids weight fraction at the vessel floor relative to the 20 weight percent pump suction maximum. The ratio is formed such that values greater than one indicate an adequate design and lesser values indicate an inadequate design. Again, extreme values represent limits of the model (for example, solids weight fraction is limited by maximum packing, and in no physical case can $0.2/C_0$ exceed a value of 5), but as in the cloud height metric (Fig. 8b) indicate a mixing system design that is either far underpowered (for very small values) or a system that has excess mixing capacity for these conditions.

SUMMARY AND CONCLUSIONS

Pulse jet mixing (PJM) tests with noncohesive solids in Newtonian liquid were conducted at three geometric scales to support the design of mixing systems for the Hanford Waste Treatment and Immobilization Plant. The test data were used to develop mixing models. The models predict the cloud height (the height to which solids will be lifted by the PJM action) and the critical suspension velocity (the minimum velocity needed to ensure all solids have been lifted from the floor). From the cloud height estimate, the concentration of solids near the vessel floor was estimated. Results of these calculations show that a number of the solids containing vessels would have difficulty suspending design solids loadings of expected waste feed.

REFERENCES

[1] Meyer PA, et al. 2009. *Pulse Jet Mixing Tests with Non-Cohesive Solids.* PNNL-18098 (WTP-RPT-182) Rev. 0, Pacific Northwest National Laboratory, Richland, WA.

[2] Bamberger JA, et al. 2009. "Scaled Experiments Evaluating Pulse Jet Mixing of Slurries." *Proceedings of IMECE2009 ASME International Mechanical Engineering Congress and Exposition* (IMECE2009-12264). American Society of Mechanical Engineers, New York.

[3] Bamberger JA, et al. 2009. "Evaluating Concentration Profiles During Unsteady Mixing." *Proceedings of the ASME 2009 Fluids Engineering Division Summer Meeting (FEDSM-78585)*. American Society of Mechanical Engineers, New York.

[4] Bamberger JA, et al. 2009. "Insitu Measurement Techniques for Characterizing Pulse Jet Mixing of Slurries." *Proceedings of IMECE2009 ASME International Mechanical Engineering Congress and Exposition* (IMECE2009-12265). American Society of Mechanical Engineers, New York.

[5] Zwietering TN. 1958. "Suspending of Solid Particles in Liquid by Agitators." *Chemical Engineering Science,* 8:244-253.

[6] Bontha JR, GR Golcar, and N Hannigan. 2000. *Demonstation and Optimization of BNFL's Pulsed Jet Mixing and RFD Sampling Systems Performance Using NCAW Simulant.* PNWD-3054 (BNFL-RPT-048) Rev. 0, Battelle – Pacific Northwest Division, Richland, Washington.

[7] Bontha JR, TE Michener, DS Trent, JM Bates, and MD Johnson. 2003. *Development and Assessment of the TEMPEST CFD Model of the Pulsed Jet Mixing Systems.* PNWD-3261 (WTP-RPT-061) Rev. 0, Battelle – Pacific Northwest Division, Richland, Washington.

[8] Bontha JR, JM Bates, CW Enderlin, and MG Dodson. 2003. *Large Tank Experimental Data for Validation of the FLUENT CFD Model of Pulsed Jet Mixers.* PNWD-3303 (WTP-RPT-081) Rev. 0, Battelle – Pacific Northwest Division, Richland, Washington.

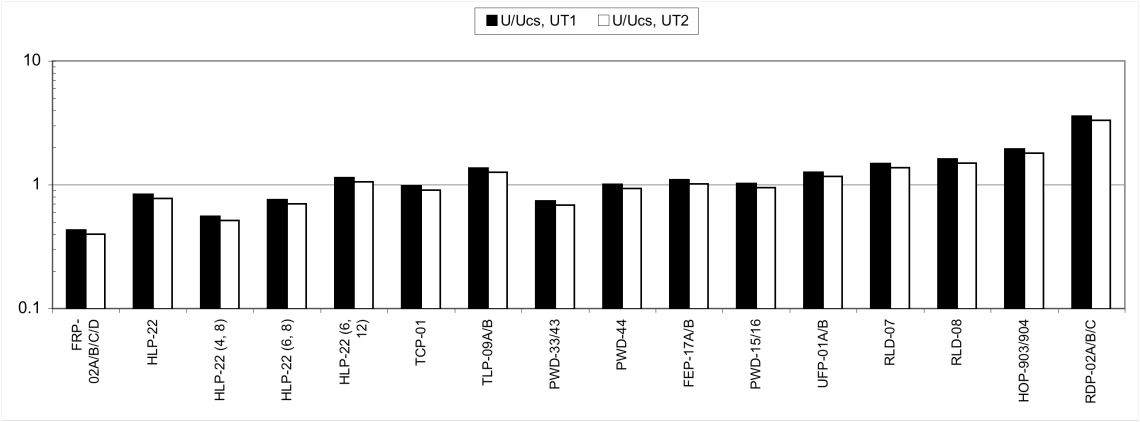

a. Critical suspension velocity metric ($U_{T1}=U_{bar53}$, $U_{T2}=U_{bar69}$)

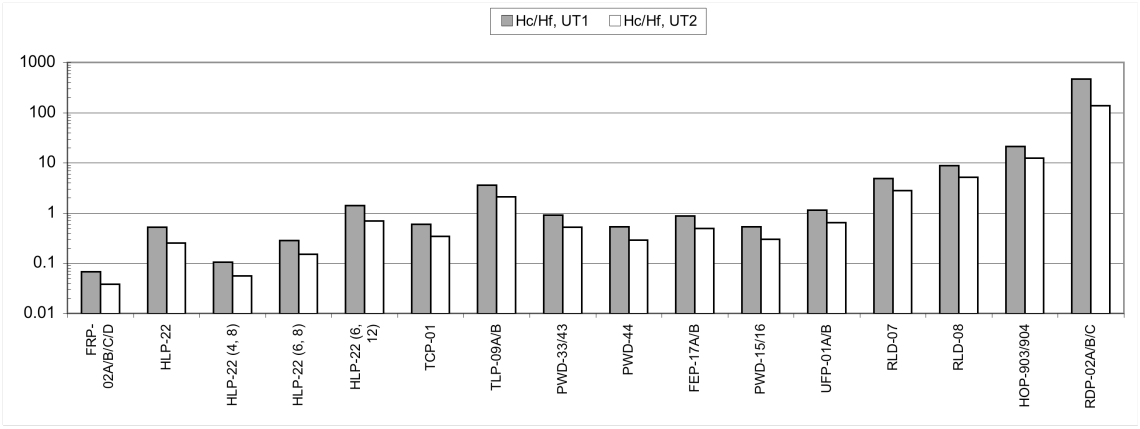

b. Cloud height ($U_{T1}=U_{bar53}$, $U_{T2}=U_{bar69}$)

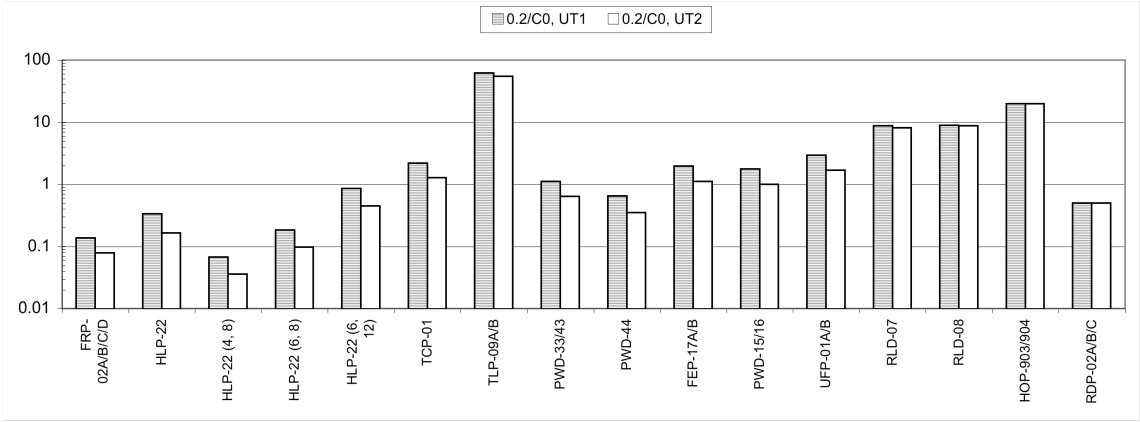

c. Concentration metric ($U_{T1}=U_{bar53}$, $U_{T2}=U_{bar69}$)

Fig. 8. Model predictions for a selection of WTP solids containing vessels using representative minimum and maximum average settling velocities ($U_{T1} = U_{bar53} = 2.2$ mm/s; $U_{T2} = U_{bar69} = 3.3$ mm/s). Results for HLP-22 are shown for four cases with nozzle diameter and discharge velocity in parentheses (inches, m/s). The unlabelled case is for the baseline HLP-22 configuration (4-inch nozzle and 12 m/s discharge velocity).